Quasi-Continuous Wave Pumped Slab Laser Based on Nd:CTGS Crystal

Shutong Yang, Chuanrui Zhao, Pingzhang Yu, and Zhengping Wang

***Abstract*—A slab laser based on Nd:CTGS crystal was reported for the first time. With a quasi-continuous wave semiconductor laser as the pump source, the maximum average output power reached 7.01 W, with a wavelength of 1064.5 nm, a single-pulse energy of 35 mJ, and a slope efficiency of 31%. Using a Cr^{4+}:YAG crystal as the saturable absorber, the maximum average output power was 2.52 W, corresponding to a single-pulse energy of 1.26 mJ, a pulse duration of 37.2 ns, and a peak power reaches 33.9 kW. This work provides a good way to obtain pulsed slab lasers with simple structure and excellent performance, which are expected to be utilized in many fields like the photovoltaic industry, glass processing, tool manufacturing, mechanical engineering, and scientific research.**

***Index Terms*—Passively Q-switched, slab laser, Nd:CTGS crystal.**

I. Introduction

SOLID-STATE lasers have the advantages of high conversion efficiency, compact and solid structure, uniform beam, etc., and have been widely used in industry, military, medicine, and other fields [1], [2], [3], [4]. With the continuous progress of science and technology, solid-state lasers also develop towards higher power. The thermal effect is the main factor limiting the ability of solid-state lasers to improve output power and beam quality [5], [6], [7], [8], [9]. The slat-shaped gain mediums possess the characteristics of a blocky medium that can accommodate large mode-field spots and withstand high-peak-power pulses, but also effectively have weaker thermal stresses and thermal distortion. These advantages, combined with their large cooling surface and thin thickness, make them applicable to large-energy, high-power pulsed lasers [10]. Passively Q-switched (PQS) technology has the advantages of low cost, stable performance, and simple structure, and is an effective way to obtain high pulse repetition frequency and high peak power [9], [10]. Currently, slab solid-state pulse lasers have been used in many fields, such as optical communication, laser printing, and 5G communication technology, and have partially replaced the traditional rod-shaped and block-shaped solid-state pulse lasers. As an active ion, Nd^{3+} ion has inherent advantages, including a long upper-level lifetime, large absorption and emission cross sections, and convenience to obtain high power near-infrared laser [11], [12], [13], [14], [15], [16], [17]. However, the large emission cross-section of Nd:YVO_4 crystal also brings high pulse repetition frequency in PQS operation, resulting in a decrease in single-pulse energy and peak power. In comparison, the Nd:$Ca_3TaGa_3Si_2O_{14}$ (Nd:CTGS) crystal has a smaller emission cross-section and a longer fluorescence lifetime, which is more conducive to PQS operations [18], [19], [20]. Large-size and high-quality Nd:CTGS crystals can be obtained by the Czochralski pulling method [21]. However, the main factor limiting the output power of the laser is the thermal effect of the laser crystal, which is prone to thermal fracture at high pumping power. Combined with the theoretical analysis of the heat transfer process and critical power for the thermal fracture of the laser crystal [22], [23], increasing the heat dissipation area of the crystal is a way to increase the output power of the laser, so the lath laser medium is more advantageous. Conventional lasers use continuous pumping sources, the conversion efficiency of light and light is low, and the thermal effect is more obvious, selecting the appropriate quasi-continuous pumping source is also an effective way to improve the performance of the laser [19], [24], [25].

In this paper, we demonstrate an end-pumped slab Nd:CTGS laser for the first time. The Cr^{4+}:YAG crystal with an initial transmittance of 96% was used as the PQS switcher, and the quasi-continuous wave (QCW) semiconductor laser with a repetition frequency of 200 Hz was used as the pump source, which greatly reduced the thermal effect. The 1064.5 nm laser exhibited an average output power of 2.52 W, a single-pulse energy of 1.26 mJ, and a peak power of 33.9 kW. It provides a good choice for the fabrication of pulsed solid-state lasers with a simple structure and excellent performance.

II. Experimental Set-Up

A PQS laser based on slab Nd:CTGS crystal was equipped, and the schematic diagram of the experimental setup was shown in Fig. 1. The pump source was a QCW semiconductor laser with a center wavelength of 808 nm and a pulse width of 200 μs. A plano-convex cylindrical lens with a focal length of 150 mm was used to focus the strip pump light on the Nd:CTGS crystal. As

Manuscript received 11 January 2024; revised 16 February 2024; accepted 22 February 2024. Date of publication 29 February 2024; date of current version 14 March 2024. This work was supported in part by the Key Research and Development Program of Shandong Province under Grant 2022CXGC010104, in part by the Major Basic Research Project of the Natural Science Foundation of Shandong Province under Grant ZR2023ZD02, and in part by the National Natural Science Foundation of China under Grant 61975096. *(Corresponding author: Zhengping Wang.)*

Shutong Yang is with the Crystrong Optoelectronic Technology Company, Ltd, Jinan 250109, China (e-mail: yst79@126.com).

Chuanrui Zhao, Pingzhang Yu, and Zhengping Wang are with the State Key Laboratory of Crystal Materials, Shandong University, Jinan 250100, China (e-mail: chuanruizhao@163.com; oct753951@163.com; zpwang@sdu.edu.cn).

Digital Object Identifier 10.1109/JPHOT.2024.3371466

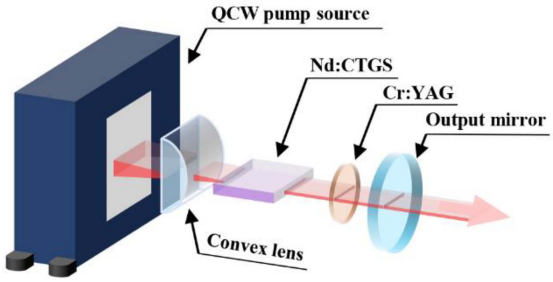

Fig. 1. Experimental setup of the PQS slab laser.

a trigonal crystal, the Nd:CTGS sample was processed along the Z-axis, with a Nd^{3+} doping concentration of 0.5 at.%, and geometric dimensions of 10 mm× 1 mm × 11 mm. The doping concentration is an optimized parameter according to our previous experience in crystal growth and laser experiments, and the crystal dimensions are designed based on the spot size of the strip pump source used in this experiment, which are 10 mm × 400 μm after focusing. The front end of the crystal was coated with a dielectric film that was highly transmissive to 0.8 μm and highly reflective to 1.06 μm, and the other end of the crystal was coated with a dielectric film that was highly reflective to 0.8 μm and antireflective to 1.06 μm. In this way, the front end-face of the Nd:CTGS crystal served as the input mirror of the laser resonator, which simplified the resonator structure, reduced the intracavity loss, and improved overall laser performance. The laser crystal was wrapped with indium foil and placed in a copper block that was cooled with circulating deionized water at a temperature of 6 °C. The PQS switcher was a Cr^{4+}:YAG crystal coated with an antireflective film to 1064 nm and an initial transmittance of 96%. The output mirror is a concave mirror with a coating of 5% transmittance at 1.06 μm and a curvature radius of 500 mm. The total length of the laser cavity was about 70 mm. The pump laser is directed into the crystal from the left end of the laser cavity, and the generated laser is output from the right end. A filter with a high reflectivity of the pump light and a high transmittance of laser (T = 92% @1064 nm) was placed after the output mirror. The output power was measured by a power meter (Max 500D, Molectron Inc.). The emission spectrum was detected by an optical spectroscopy analyzer (HR 4000, Ocean Optics). The pulse performance was recorded by a digital oscilloscope (DPO 4000, Tektronix Inc.).

III. Experimental Results and Discussion

Firstly, the Cr^{4+}:YAG crystal was removed from the laser resonator, and we optimized the repetition frequency of the pump source in the QCW operation mode to obtain the most excellent laser performance. During the experiment, the repetition frequency of the pump source was set to be 100 Hz, 200 Hz, 300 Hz, 400 Hz, and 500 Hz, respectively, and the corresponding slope efficiencies were 34.4%, 31%, 29.7%, 28.9%, and 24%, respectively. The maximum output laser powers were 4.26 W, 7.01 W, 6.33 W, 6.55 W, and 5.34 W, respectively. The relationship between the output power of the QCW laser and the input pump power is shown in Fig. 2. Generally, as the repetition frequency of the pump source increases, the initial slope efficiency of the output laser power and the maximum output power are subsequently reduced, i.e., the optical-to-optical conversion efficiency decreases. However, when the pump source is operated at a lower repetition frequency (100 Hz), the crystal is more likely to reach saturation, which results in the laser operating in a reduced power range and a smaller maximum output laser power. This is due to that the laser duty cycle of the pump source is low for lower repetition frequency operation, the peak power of the pump output is higher and the crystal thermal effect is more obvious under the same average input power. If the input pump power is further elevated after the slope efficiency of the output power curve begins to decrease, the higher thermal effect can cause damage to the crystal or even produce a thermal fracture of the crystal. Based on the theoretical analysis of the heat transfer process and critical power of the thermal fracture of laser crystals [22], [23], in addition to increasing the heat dissipation area of the crystal, choosing the appropriate pump repetition frequency is also an effective way to improve the output power of the laser. As a result, when the repetition frequency of the pump source is 200 Hz, the laser has the largest output power, corresponding to a single-pulse energy of 35 mJ.

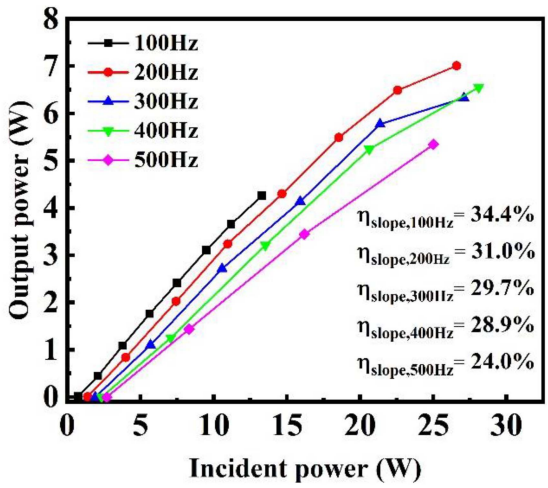

Fig. 2. Relationship between the output power of the QCW laser and the input pump power when the pump source is operated at different repetition frequencies.

For passively Q-switched operation, the repetition frequency of the pump source was fixed at 200 Hz and the duty cycle of the laser was 4%. A Cr^{4+}:YAG crystal was inserted into the laser cavity to obtain a stable PQS pulsed laser output, and the laser performance is shown in Fig. 3. The number of PQS pulses (NPP) in a single pump pulse and pulse duration ($\Delta\tau$) were measured in the experiment. The total number of pulses per unit time (TNP) is the product of the pump source's repetition frequency and the NPP. The single-pulse energy (Eout) is calculated by Pout/TNP, and the peak power (Ppeak) is calculated by Eout/$\Delta\tau$. As can be seen from Fig. 3(a)–(c), the input pump power threshold of PQS laser output is 1.39 W. As the input pump power increases, the average output power increases linearly, the

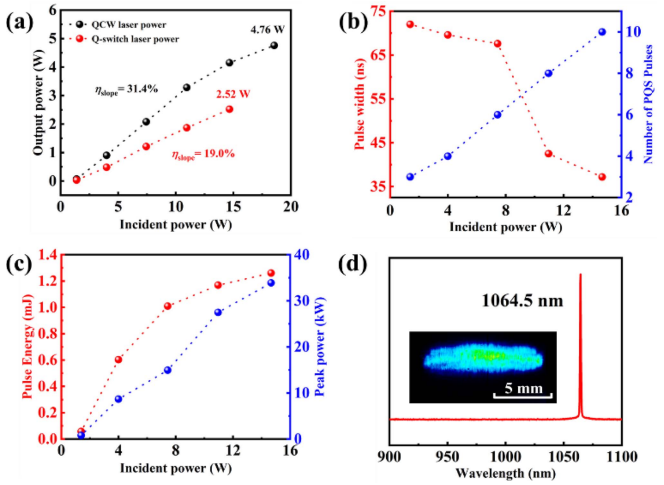

Fig. 3. Performance of PQS laser based on QCW pumping (200 Hz). (a) Output power. (b) Pulse width and the number of pulses under each pump pulse. (c) Single-pulse energy and peak power. (d) The laser emission spectrum and the inset show the facula profile of the strip laser.

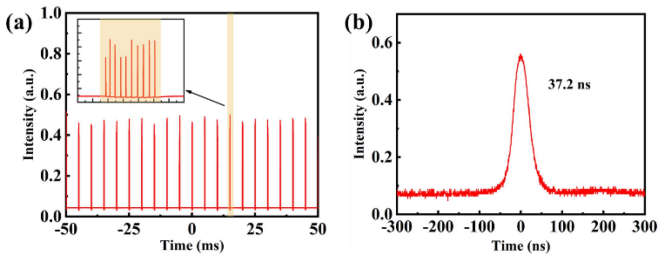

Fig. 4. (a) Pulse sequence at the maximum input pump power of 14.67 W, and the inset shows the PQS pulse sequence at a single pump pulse. (b) The single pulse waveform of the PQS laser.

pulse duration decreases from 72 ns to 37.2 ns, and the number of PQS pulses under a single pump pulse increases from 3 to 10. When the input pump power is 14.67 W, the maximum power is 2.52 W and the optical conversion efficiency is 17.2%. At this point, both the single-pulse energy and peak power reach their maximum values, which are 1.26 mJ and 33.9 kW, respectively. When the input pump power continues to increase, the pulse time interval is no longer uniform, and the output reaches saturation. When the input pump power is reduced to the normal working interval (1.39–14.67 W), the pulse laser output waveform returns to stability, indicating that the laser crystal and the saturable absorber are not damaged. The laser emission spectrum is shown in Fig. 3(d), and the output laser wavelength is 1064.5 nm. The inset of Fig. 3(d) shows the facula profile of the slab PQS laser. The length of the facula is 10 mm and the width is 2.5 mm.

Fig. 4 shows the pulse properties at the maximum input pump power of 14.67 W, i.e., the PQS pulse sequence, and the single pulse waveform of the PQS laser. The laser pulse sequence is neat and stable, and the pulse duration is 37.2 ns.

Table I lists the characteristics of ~1 μm PQS lasers based on CTGS and CNGS crystals with Cr^{4+}:YAG crystals as saturable absorbers. Compared with bulk crystals and continuous-wave pump sources, the use of slatted laser crystal and QCW pump

TABLE I
CHARACTERISTICS OF ~1 μM PQS LASERS BASED ON CTGS AND CNGS CRYSTALS WITH Cr^{4+}:YAG CRYSTAL AS SATURABLE ABSORBER

Laser Crystal	Crystal Size (mm^3)	Pump style	Wavelength (nm)	Pout (PQS)	Pulse energy (μJ)	Peak power (kW)	Ref.
Yb:CNGS	4×3×3	CW	1015.8	1.4 W	62.2	14	[26]
Nd:CTGS	3×3×6	CW	1065	1.6 W	45.7	5.4	[18]
Nd:CTGS	10×1×11	QCW (200 Hz)	1064.5	2.52 W	1260	33.9	This work

CW: Continuous wave

source increases the output power of PQS pulse laser by about 58%, the single-pulse energy by 28 times, and the peak power by 6 times. It can be seen that the PQS laser based on the slatted Nd:CTGS crystal and the QCW pump source has the characteristics of large single-pulse energy and high peak power.

IV. CONCLUSION

In this paper, a PQS slab laser based on Nd:CTGS crystal is reported. A Cr^{4+}:YAG crystal with an initial transmittance of 96% is used as the SA, and a QCW semiconductor laser with a repetition frequency of 200 Hz is employed as the pump source. The maximum average output power is 2.52 W, the single pulse energy is 1.26 mJ, and the peak power is 33.9 kW. These results show that Nd:CTGS crystal is an excellent slab laser medium, which is favorable for fabricating simple, miniaturized, and high-power pulsed solid-state lasers and is expected to be widely used in the future.

REFERENCES

[1] Z. Tian, H. Cheng, P. Xu, X. Zhang, and S. Fu, "Laser output of the radial-slab solid-state laser," *Chin. Opt. Lett.*, vol. 11, no. 4, 2013, Art. no. 041404.
[2] Z. Chen et al., "A CRISPR/Cas12a-empowered surface plasmon resonance platform for rapid and specific diagnosis of the omicron variant of SARS-CoV-2," *Nat. Sci. Rev.*, vol. 9, no. 8, 2022, Art. no. nwac104.
[3] F. Zheng et al., "A highly sensitive CRISPR-empowered surface plasmon resonance sensor for diagnosis of inherited diseases with femtomolar-level real-time quantification," *Adv. Sci.*, vol. 9, 2022, Art. no. 2105231.
[4] T. Xue et al., "Ultrasensitive detection of miRNA with an antimonene-based surface plasmon resonance sensor," *Nature Commun.*, vol. 10, no. 1, 2019, Art. no. 28.
[5] A. Giesen and J. Speiser, "Fifteen years of work on thin-disk lasers: Results and scaling laws," *IEEE J. Sel. Topics Quantum Electron.*, vol. 13, no. 3, pp. 598–609, May/Jun. 2007.
[6] S. Lee, M. Yuan, B. H. Cha, C. J. Kim, S. Suk, and H. S. Kim, "Stability analysis of a diode-pumped, thermal birefringence-compensated two-rod Nd:YAG laser with 770-W output power," *Appl. Opt.*, vol. 41, no. 27, pp. 5625–5631, 2002.
[7] P. Zhu et al., "Diode end-pumped high-power Q-switched double Nd:YAG slab laser and its efficient near-field second-harmonic generation," *Opt. Lett.*, vol. 33, no. 19, pp. 2248–2250, 2008.
[8] Y. Wang, F. Chen, M. Wang, and J. Xu, "Scattering loss and efficiency of the multi-pass mini-slab Nd:YAG ceramic lasers," *Chin. Opt. Lett.*, vol. 9, no. 2, 2011, Art. no. 021402.
[9] X. Cheng, Z. Wang, F. Chen, and J. Xu, "Edge-pumped passively Q-switched thin Nd:YAG slab lasers," *Chin. Opt. Lett.*, vol. 6, no. 5, pp. 364–364, 2008.
[10] Z. Wang, J. Xu, and W. Chen, "High-power passively Q-switched ultra-thin slab lasers," *Chin. Opt. Lett.*, vol. 5, pp. S36–S38, 2007.
[11] G. A. Henderson, "A computational model of a dual-wavelength solid-state laser," *J. Appl. Phys.*, vol. 68, pp. 5451–5455, 1990.
[12] Z. Wang et al., "Passively Q-switched dual-wavelength laser output of LD-end-pumped ceramic Nd:YAG laser," *Opt. Exp.*, vol. 17, no. 14, pp. 12076–12081, 2009.
[13] Y. Zhao, H. Yu, Z. Wang, H. Zhang, X. Xu, and J. Wang, "Homogeneous and inhomogeneous spectrum broadening in Nd^{3+}-doped mixed vanadate crystals," *Opt. Mater*, vol. 17, no. SI, pp. 78–85, 2017.

[14] M. Wang, F. Zhang, Z. Wang, Z. Wu, and X. Xu, "Passively Q-switched Nd^{3+} solid-state lasers with antimonene as saturable absorber," *Opt. Exp.*, vol. 26, no. 4, pp. 4085–4095, 2018.
[15] C. Tang et al., "Optimization design of Nd:YVO_4 slab laser amplifier with grazing incidence," *Chin. J. Lasers*, vol. 44, 2017, Art. no. 1201003.
[16] S. Xu et al., "Experimental study of grazing incidence slab laser amplifier with high gain," *Chin. J. Lasers*, vol. 45, 2018, Art. no. 0101008.
[17] X. Liu et al., "7 kHz sub-nanosecond microchip laser amplified by a grazing incidence double pass slab amplifier," *Chin. Opt. Lett.*, vol. 19, no. 2, 2021, Art. no. 021403.
[18] Y. Zhou, Z. Wang, F. Chen, Y. Liu, and X. Xu, "Continuous-wave and passively Q-switched c-cut Nd:CTGS laser," *Proc. SPIE*, vol. 11068, pp. 399–404, 2019.
[19] C. Zhao, P. Yu, Z. Wang, Y. Liu, F. Yu, and X. Xu, ">10 kW peak power self-frequency doubling laser," *Laser Phys. Lett.*, vol. 20, 2023, Art. no. 045001.
[20] Y. Zhou, Z. Wang, F. Chen, F. Yu, and X. Xu, "1 kW peak power self-frequency-doubling microchip laser," *IEEE Photon. J.*, vol. 11, no. 2, Apr. 2019, Art. no. 1501405.
[21] F. Chen et al., "Crystal growth and characterization of CTGS and Nd:CTGS for self-frequency-doubling applications," *CrystEngComm*, vol. 16, pp. 10286–10291, 2014.
[22] S. Wang and L. Sang, "Diode-pumped Nd:YCOB self-frequency-doubling green laser at 530 nm," *Laser Phys.*, vol. 21, 2011, Art. no. 1347.
[23] J. Xia et al., "Pure-three-level Yb:GdCOB CW laser at 976 nm," *Opt. Lett.*, vol. 43, 2018, Art. no. 3981.
[24] C. Zhao, Z. Wang, P. Yu, F. Zhang, and X. Xu, "High performance 1.9 μm passively Q-switched bulk laser with Germanene as a saturable absorber," *Opt. Exp.*, vol. 31, no. 15, pp. 3981–3984, 2023.
[25] C. Zhao, Z. Wang, G. Liu, P. Yu, and X. Xu, "Infrared saturable absorption properties of tungstenene nanosheets for passively Q switched 1.9 μm solid-state laser," *Amer. Chem. Soc. Appl. Nano Mater.*, vol. 6, pp. 19499–19507, 2023.
[26] X. Zhang et al., "Passive Q switching of Yb:CNGS lasers by Cr^{4+}:YAG and V3+:YAG saturable absorbers," *Appl. Opt.*, vol. 57, no. 28, pp. 8236–8241, 2018.